

Gripping mechanisms in current wood harvesting machines

Journal:	<i>Frontiers of Mechanical Engineering</i>
Manuscript ID:	Draft
Manuscript Type:	Original Article
Date Submitted by the Author:	n/a
Complete List of Authors:	GOUBET, David; Institut Pascal, FAUROUX, Jean-Christophe; French Institute for Advanced Mechanics, Institut Pascal Gogu, Grigore; French Institute for Advanced Mechanics, Institut Pascal
Keywords:	structural synthesis, parallel mechanisms, gripping mechanisms, wood harvesting, harvesting heads
Speciality:	Design Methodology, Mechanisms & Robotics

SCHOLARONE™
Manuscripts

Gripping mechanisms in current wood harvesting machines

Authors:

D. Goubet, J.C. Fauroux, G. Gogu – Clermont University, French Institute for Advanced Mechanics (IFMA), Institut Pascal, UMR 6602 UBP/CNRS/IFMA, BP 10448, F-63000 Clermont-Ferrand, France, e-mail: david.goubet@ifma.fr | jean-christophe.fauroux@ifma.fr | grigore.gogu@ifma.fr

Abstract

This paper focuses on the structural synthesis of gripping mechanisms used in the mechanization of the harvesting process. The importance of the gripping function in current devices like harvesting heads is underlined. This function is performed with several typical mechanisms which are listed and described in this article. This study distinguishes two kinds of planar gripping mechanisms mainly used in opening and closing the rollers: five concentric and two lateral ones. Both kinds have advantages and drawbacks. So a third kind of hybrid mechanism has been designed in order to orientate the axis of the rollers during gripping motion in order to combine concentric and lateral gripping advantages. Two planar and one spatial existing mechanisms are described. The last part of this paper presents a structural synthesis of such a spatial parallel mechanism by using the structural parameters and the general formulae established by the third author. Nine kinematic diagrams of spatial parallel mechanisms are provided.

Keywords

Structural synthesis – parallel mechanisms – gripping mechanisms – wood harvesting – harvesting head.

1 Introduction

1.1 Wood harvesting

Wood harvesting is a part of the forest exploitation activities. It consists of two main operations which are “felling” and “processing”. The “felling” operation aims to cut the tree as close as possible from the ground and orientate its fall. The “processing” one can be decomposed in two phases: “delimiting” and “cutting to length”. At the end, the felled tree is transformed into calibrated logs without branches ready to be transported to the storage area.

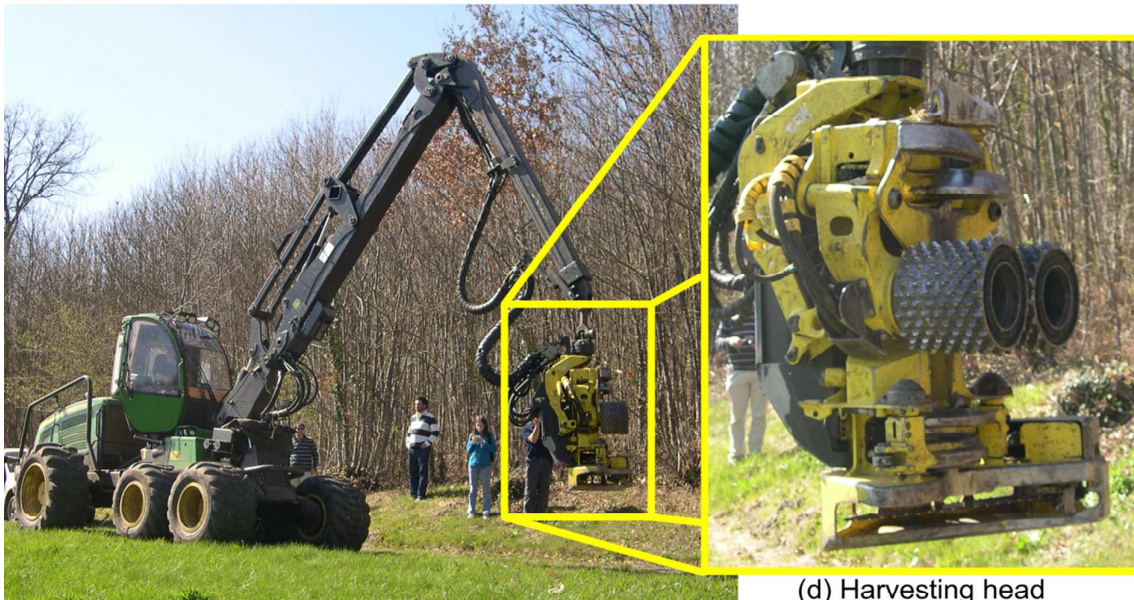
These operations have been performed manually for a long time and nowadays, especially in the broadleaved trees exploitation, they are still mainly done with motorized chain saws (Figure 1-a) [1], despite the strong actual trends of mechanization in the harvesting process. The first processing machine (Figure 1-b) [2] appeared in the seventies. Then, the first “all-in-one” harvesting heads (Figure 1-d) [3] mounted on a wood harvester (Figure 1-c) [4] arrived in the nineties. In 2009, about 800 wood harvesting machines worked in France [5].



(a) Motorized chain saw
STIHL MS 660



(b) Processing machine
SIFER 103C



(c) Wood harvester
JOHN DEERE 1170 E

(d) Harvesting head
JOHN DEERE H752HD

Figure 1: Mechanized devices used in wood harvesting

1.2 All-in-one harvesting head

1.2.1 Description of the system functioning

The main components of an all-in-one harvesting head are listed in Figure 2.

The all-in-one harvesting head is moved towards the standing tree by the articulated boom of the vehicle. Then, it grips the tree against the frame (1) using the upper knives (2 and 2'), the lower knives (5 and 5') and the rollers (3 and 3') supported by the roller arms (4 and 4'). Once the head is locked on the tree, the chain saw (6) is actuated in order to cut it down. The tilt support (0) allows the frame to follow the tree during its fall without dropping it. When the tree is in a horizontal position, the rollers (3 and 3') give it a translational motion while the upper knives (2 and 2') cut the branches. During this delimiting operation, a device measures the diameter and the length of the tree trunk which is passed through the head. Comparing these data to the log specifications, the operator chooses the right length for the log to be generated. Then the rollers stop to turn when the chain saw is

right positioned and the chain saw (6) cuts the well calibrated log. Delimiting and cutting to length phases are successively performed until the tree is all transformed into logs.

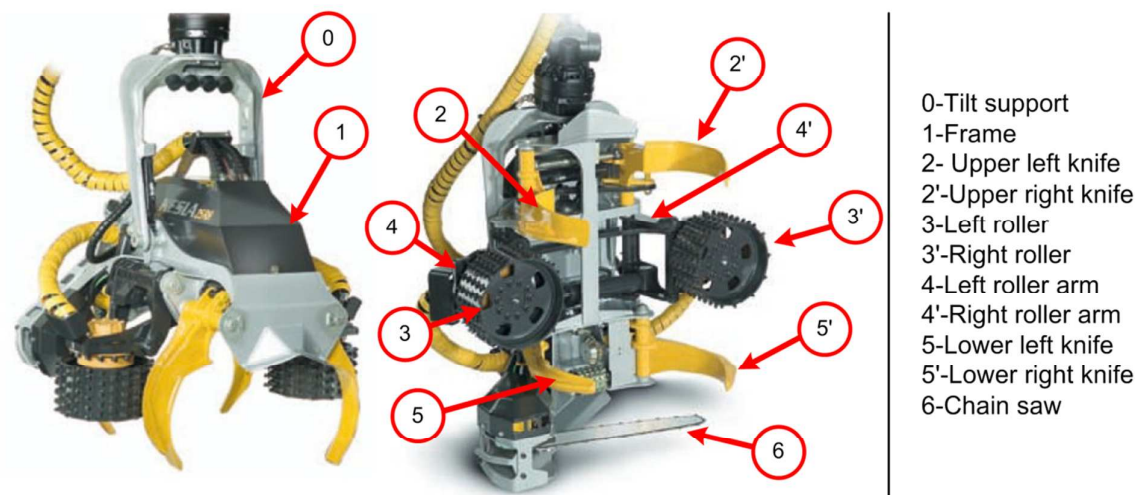


Figure 2: Harvesting head KESLA 25 RH [6]

1.2.2 Function analysis

The importance of the gripping capacity is underlined in the simplified FAST diagram (Figure 3) showing the functional decomposition of an all-in-one harvesting head.

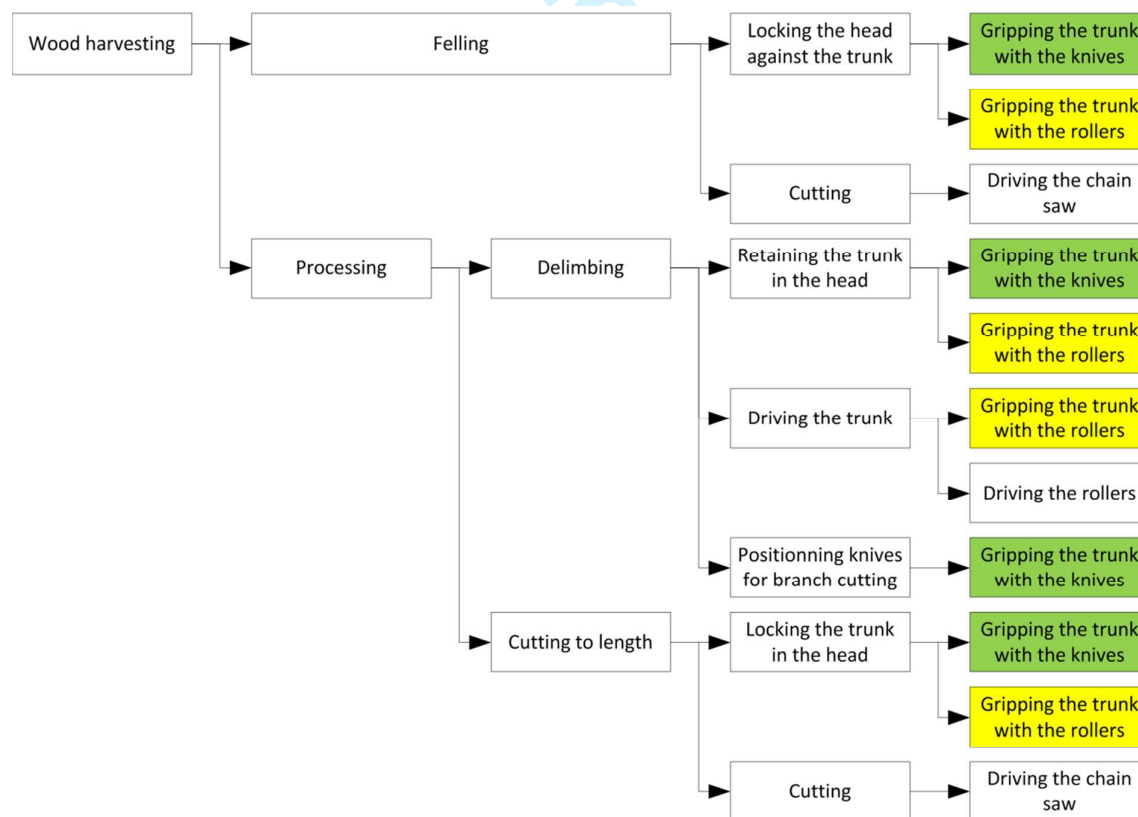


Figure 3: Simplified FAST diagram of an all-in-one harvesting head and importance of the gripping capacity

2 The gripping function

2.1 Its aim

2.1.1 *The normal effort*

The gripping function creates an effort normal to the trunk surface. This effort is useful for several others actions. The normal effort generated by the motorized rollers allows them to apply a tangential propelling effort to the trunk in order to make it move through the harvesting head. The normal effort generated by the upper knives allows them to cut the branches at their base without sliding on them. The normal efforts generated by both the rollers and the knives allow the head to be clamped on the trunk during the felling and cutting to length operations.

2.1.2 *The head/trunk orientation*

The gripping forces performed by both the knives and the rollers guide the trunk in its translational motion through the harvesting head, during the delimiting operation. By this way, the knives are well oriented in order to cut the branches as close as possible from their base without going into the log wood.

The right head/trunk orientation is also important during the static operations like felling and cutting to length. It allows fixing the local axis of the trunk in order to actuate the chain saw in a perpendicular plane.

3 The gripping mechanisms

The gripping function is performed by the knives and the arms supporting the rollers. Three kinds of gripping mechanisms are commonly used to actuate these devices and then concretely achieve this function:

- mechanisms with concentric gripping motion,
- mechanisms with lateral gripping motion,
- mechanisms with a hybrid gripping motion.

Lateral and hybrid gripping mechanisms are only used to move the roller arms. The knives are only actuated by concentric motion.

3.1 Concentric gripping mechanisms

Figure 4 presents a general simplified kinematic diagram of an all-in-one harvesting head and its main components. On this diagram, both the knives and the roller arms have a concentric gripping motion. The actuators are not illustrated.

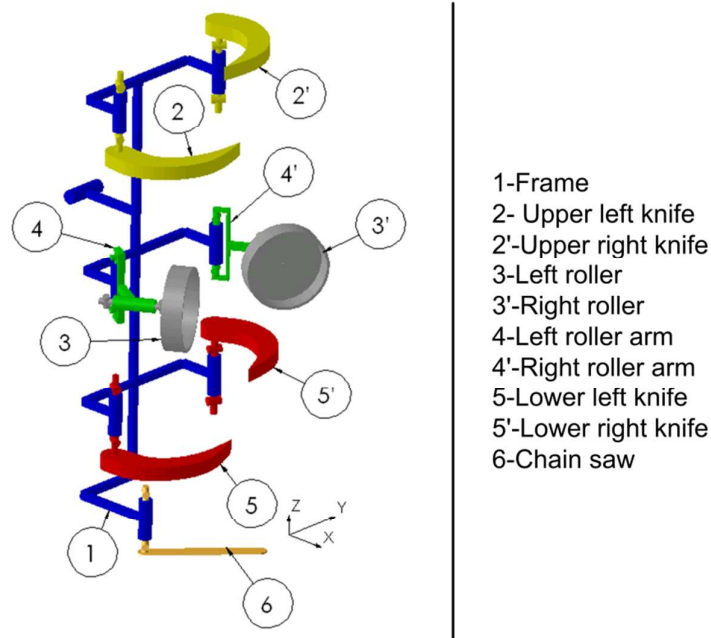


Figure 4: Simplified kinematic diagram of an all-in-one harvesting head

The mechanisms listed below are represented in the (X, Y) plane, according to the reference frame shown in Figure 4. The conventional representation and naming of the kinematic pairs used in our paper are presented in Annex 1.

3.1.1 Concentric gripping mechanisms with single actuator

In such a mechanism (Figure 5), the gripping motion of both the right and the left knives are not coupled: the angle between the left knife and the frame is not necessarily the same as the angle between the right one and the frame. Then, without the trunk, the mechanism behaves like a four bar linkage with the actuator combined in the coupler link. The resulting mobility, existing for a fix position of the actuator, disappears when the trunk is clamped, that is when the two knives are in contact with the trunk and press it against the frame.

In order to prevent the alignment issues of the trunk in the head, caused by its imperfect cylindrical form, there could be a “V” centering shape on the frame.

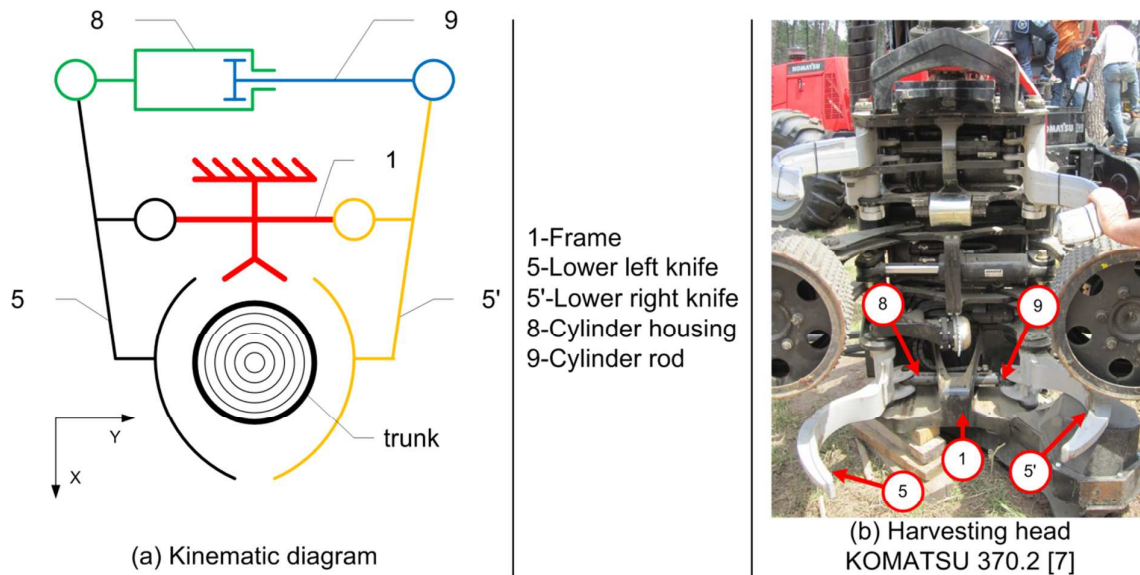


Figure 5: Lower knives moved by a concentric gripping mechanism with single actuator.

The concentric gripping mechanisms with one actuator are not used to actuate the roller arms in the actual all-in-one harvesting heads.

3.1.2 Concentric gripping mechanism with two actuators

Such a mechanism (Figure 6) uses one more actuator. Contrary to the last mechanism described in the previous section, both the actuators are linked to the frame. Each can move separately a knife.

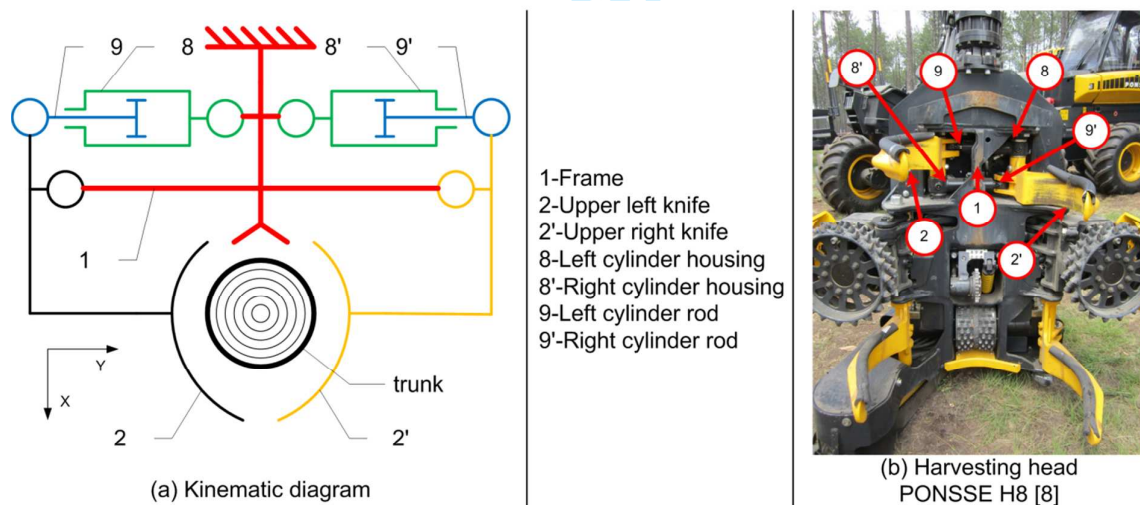


Figure 6: Upper knives moved by a concentric gripping mechanism with two actuators.

The command of the hydraulic actuators is usually performed by a three positions hydraulic valve. This valve sends some hydraulic fluid simultaneously in both actuators according to the hydraulic diagram described in Figure 7. The hydraulic fluid can be injected in the two actuators with a non-symmetric distribution. When the valve is in the central closed position, the hydraulic fluid can move from a cylinder to the other. When a cylinder rod is deployed, the rod of the other cylinder has the opposite motion. As a conclusion, this mechanism behaves like the mechanism with only one actuator.

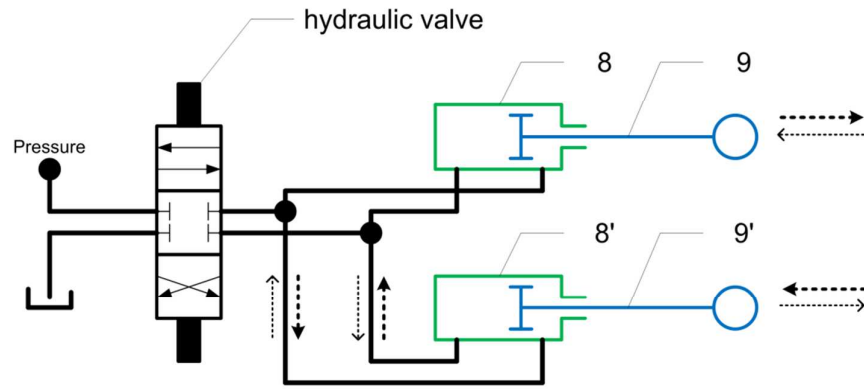


Figure 7: Hydraulic diagram of the actuator driving system.

The concentric gripping mechanism with two actuators is also used for the roller arms (Figure 8).

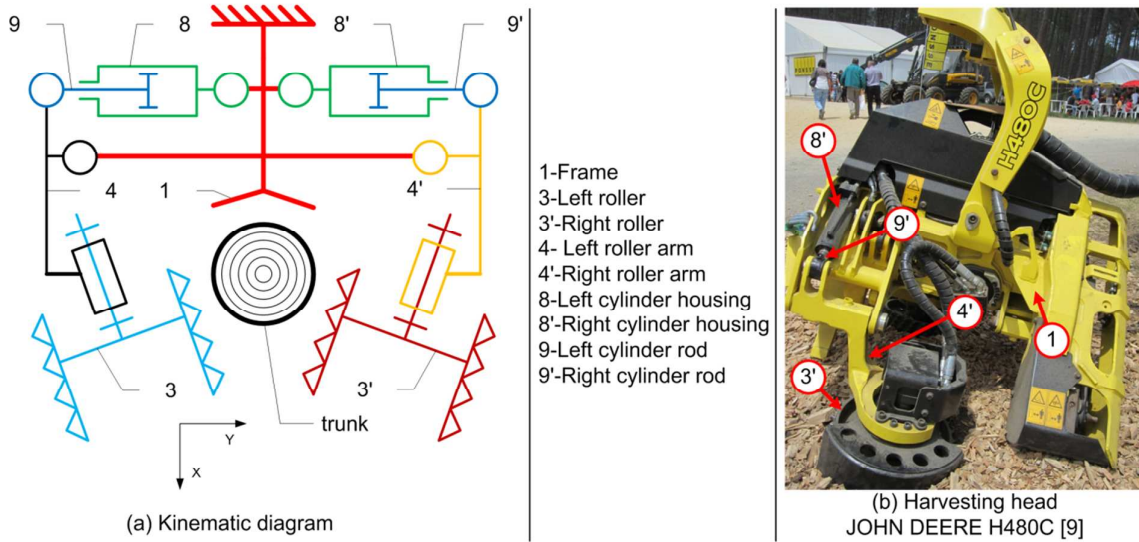


Figure 8: Roller arms moved by a concentric gripping mechanism with two actuators

3.1.3 Concentric gripping mechanism with one actuator and a coupling bar

Such a mechanism (Figure 10) uses only one actuator. A coupling bar (7) is added between the two knives or the two roller arms. Without the actuator, the mechanism behaves like a four bar linkage, having one mobility. The actuator fixes the mechanism position by suppressing this mobility.

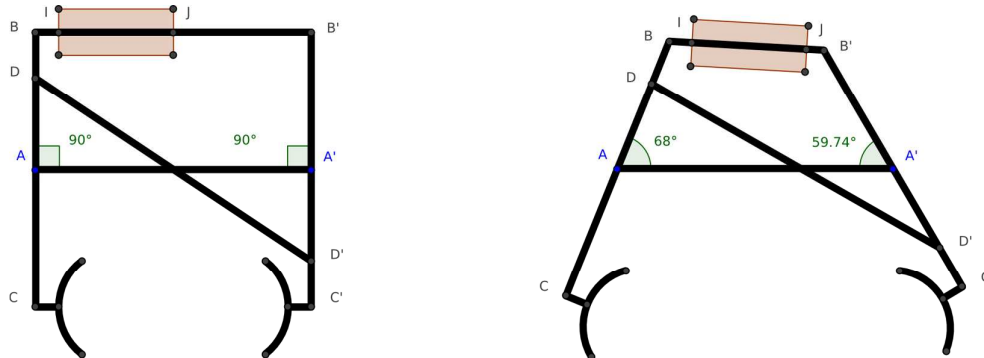


Figure 9: Geometric representation of the non-symmetric motion due to the coupling bar

The motion of the two knives or the two roller arms is not symmetric: the angle between the left component and the frame is not equal to the angle between the right one and the frame (Figure 9). However, by choosing an appropriate geometry, it is possible to obtain a behavior near the perfect symmetry.

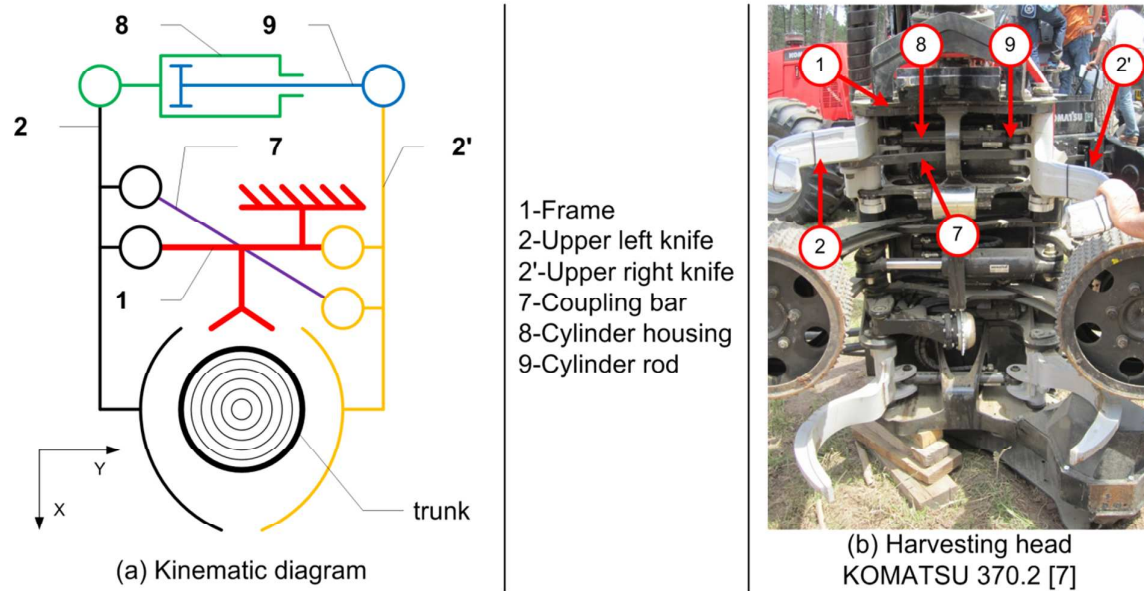


Figure 10: Upper knives moved by a concentric gripping mechanism with coupling bar

Most of the harvesting heads, using a concentric gripping mechanism for the roller arms, are equipped with a coupling bar (Figure 11).

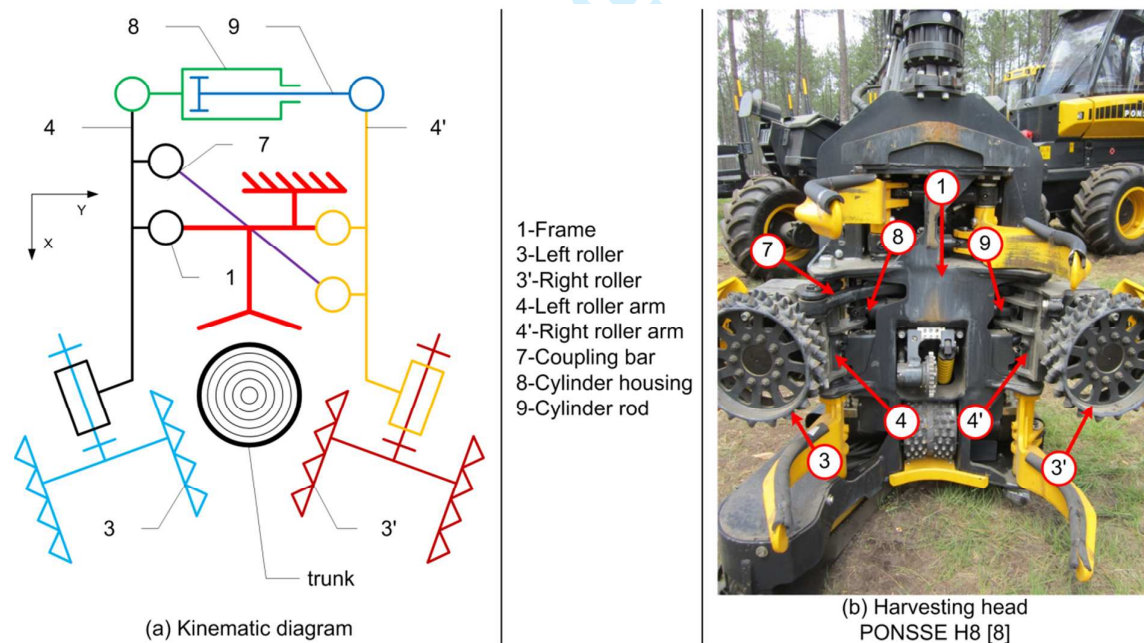


Figure 11: Roller arms moved by a concentric gripping mechanism with coupling bar.

3.1.4 Conclusions on the concentric gripping mechanisms

For each couple of components (upper knives, lower knives and roller arms), the concentric gripping mechanism positions the trunk into the harvesting head in X and Y coordinates. The addition of the three positioning stages creates an overconstrained state between the trunk and the head. So, a flexuous trunk may have some difficulties to go through such a head without locking.

Moreover, the closure position of the rollers actuated by a concentric gripping mechanism always leaves a free triangle between the frame and the rollers (Figure 12). This phenomenon does not allow gripping trunks of very small diameter.

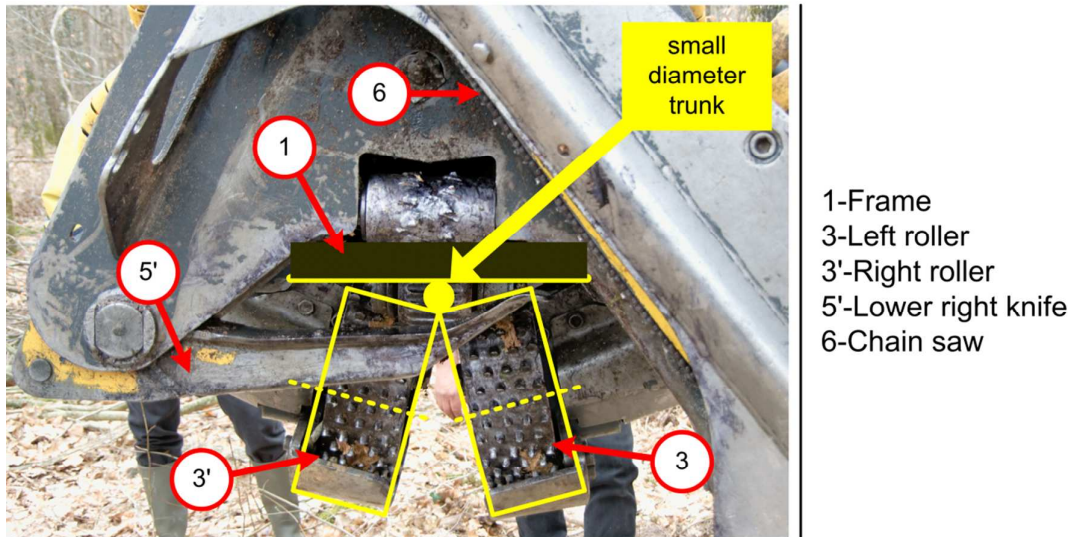
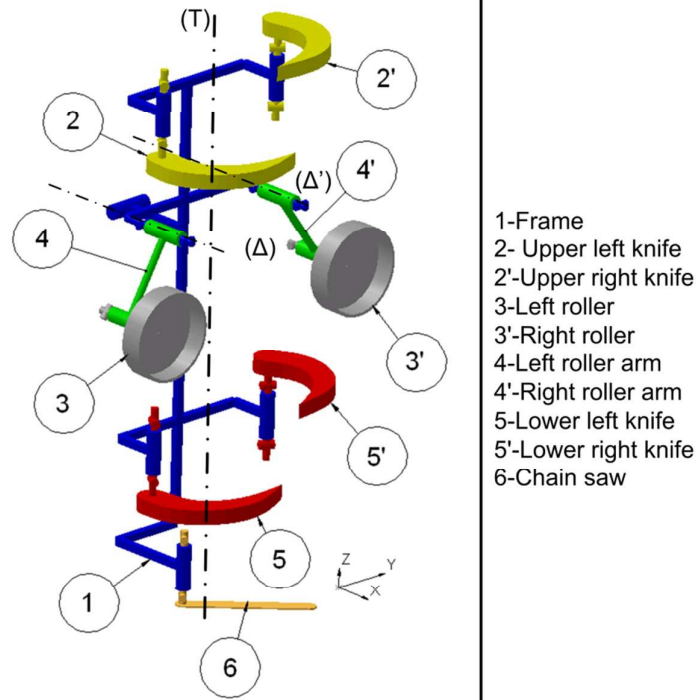


Figure 12: Rollers in closure position – free triangle.

3.2 Lateral gripping mechanisms

In order to suppress the drawbacks of the concentric gripping mechanism, described in the previous section, some of all-in-one harvesting heads purpose a lateral gripping mechanism (Figure 13). Such actuated roller arms 4 and 4' have a circular trajectory around axes (Δ) and (Δ') that are parallel together and perpendicular to the trunk axis (T).

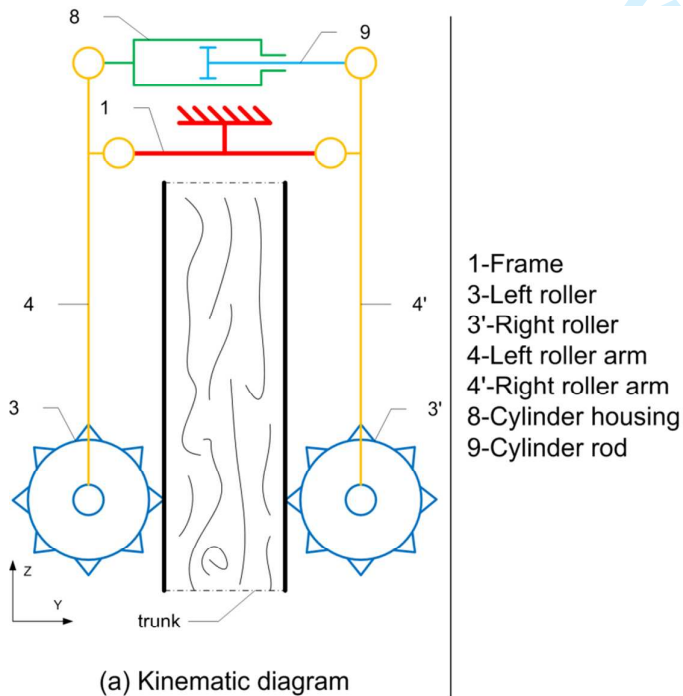


- 1-Frame
- 2- Upper left knife
- 2'-Upper right knife
- 3-Left roller
- 3'-Right roller
- 4-Left roller arm
- 4'-Right roller arm
- 5-Lower left knife
- 5'-Lower right knife
- 6-Chain saw

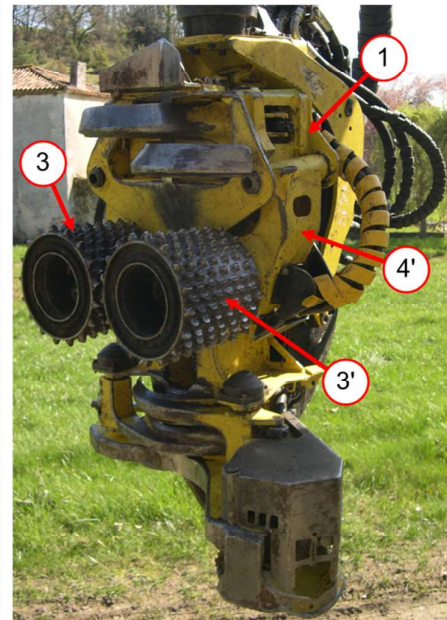
Figure 13: Simplified kinematic diagram of an all-in-one harvesting head with lateral gripping mechanism

The lateral gripping mechanisms listed below are represented in the (Y, Z) plane, according to the reference frame shown in Figure 13.

3.2.1 Lateral gripping mechanism with single actuator



- 1-Frame
- 3-Left roller
- 3'-Right roller
- 4-Left roller arm
- 4'-Right roller arm
- 8-Cylinder housing
- 9-Cylinder rod



(b) Harvesting head JOHN DEERE H752HD [3]

Figure 14: Roller arms moved by a lateral gripping mechanism with single actuator

As the concentric gripping mechanism with a single actuator, the lateral gripping mechanism also behaves like a four bar linkage. So, by a free left/right rocking motion of the roller arms, the head is able to follow a flexuous trunk.

3.2.2 Lateral gripping mechanism with two actuators

As for the concentric gripping mechanism, having one or two actuators in the lateral gripping mechanism does not change its behavior.

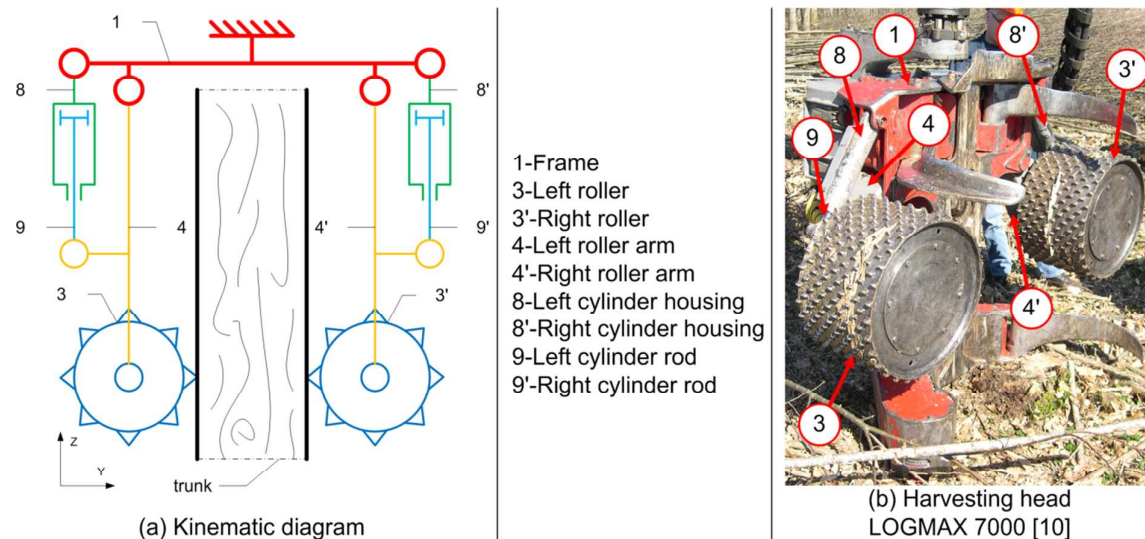


Figure 15: Roller arms moved by a lateral gripping mechanism with two actuators

3.2.3 Conclusions on the lateral gripping mechanisms

The lateral gripping mechanism is more suitable than the concentric one when the trunk is flexuous because of its free rocking motion. Contrary to the concentric gripping mechanism, the trunk is here not pressed against the frame. When the trunk and the head are in a horizontal position, the trunk is just retained in the head by the friction of the roller pins. It could be a drawback when the trunk is heavy. In this case, the trunk must be also retained and guided by the upper and lower knives.

Contrary to the concentric gripping mechanism, the clamping capacity of the lateral one is not affected by the small trunk diameter. The two rollers can roll one over the other without any free space between them.

The lateral gripping mechanism is only used for the rollers: there is no harvesting head with such a mechanism for the knives.

3.3 Hybrid gripping mechanisms

Concentric gripping mechanisms are able to retain a trunk against the frame, especially when the head is in a horizontal position. On the other side, such a mechanism does not allow to clamp a trunk which has a very small diameter.

Inversely, lateral gripping mechanisms are not able to retain a heavy trunk positioned horizontally, but they are able to clamp a very small diameter trunk.

According to the TRIZ theory, this is a typical physical contradiction: “For the rollers, a concentric gripping motion is required to retain trunks with a great diameter and a lateral gripping motion is required to clamp trunks with very small diameter.”

Such a contradiction can be solved by using innovation methods like separation upon conditions: the gripping motion (lateral or concentric) should be adapted to the trunk diameter. In other words, the gripping motion should be coupled with the closure motion of the rollers.

The mechanisms listed below are examples of marketed heads using this principle.

3.3.1 Four bar gripping mechanism

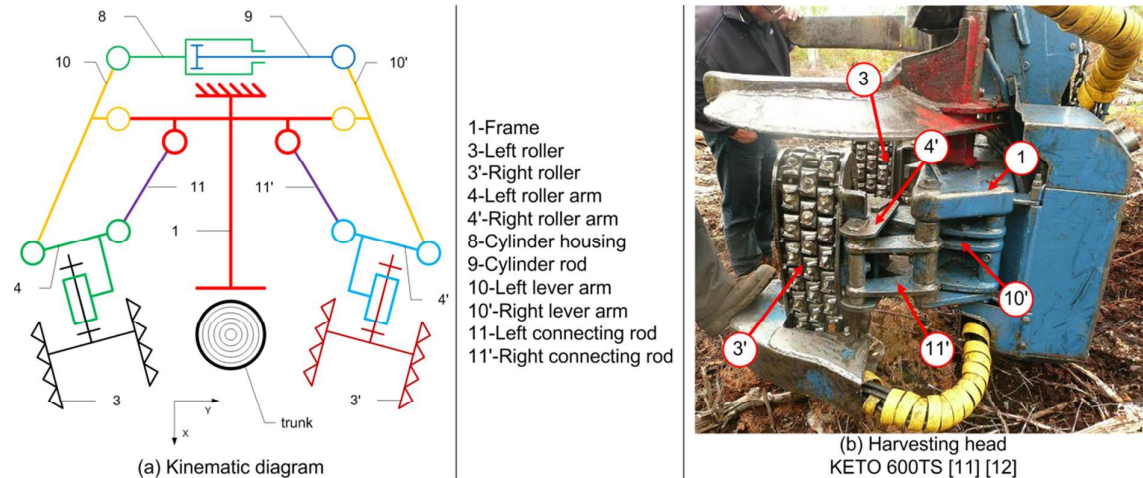


Figure 16: Arms moved by a four bar gripping mechanism. The arms 4 and 4' load (a) rollers (b) tracks

The mechanism shown in Figure 16 consists of two four bar linkages, one for each roller arms. Knowing that a four bar mechanism has one mobility, this association gives two mobilities to the resulting mechanism. Moved by only one actuator, the mechanism keeps one mobility corresponding to the left/right rocking motion.

The roller axis orientation is modified during the gripping. With an optimized length of each bar this mechanism is able to answer to the previous contradiction.

3.3.1 Cam gripping mechanism

The mechanism shown in Figure 17 looks like a concentric gripping mechanism. Roller arm 4 (respectively 4') is linked to lever arm 10 (respectively 10') by a revolute pair and to frame 1 by a sphere/plane contact pair. This last pair constitutes a cam-roller system which changes the orientation of the roller axis during the gripping.

As the previous mechanism, this one can have a left/right rocking motion.

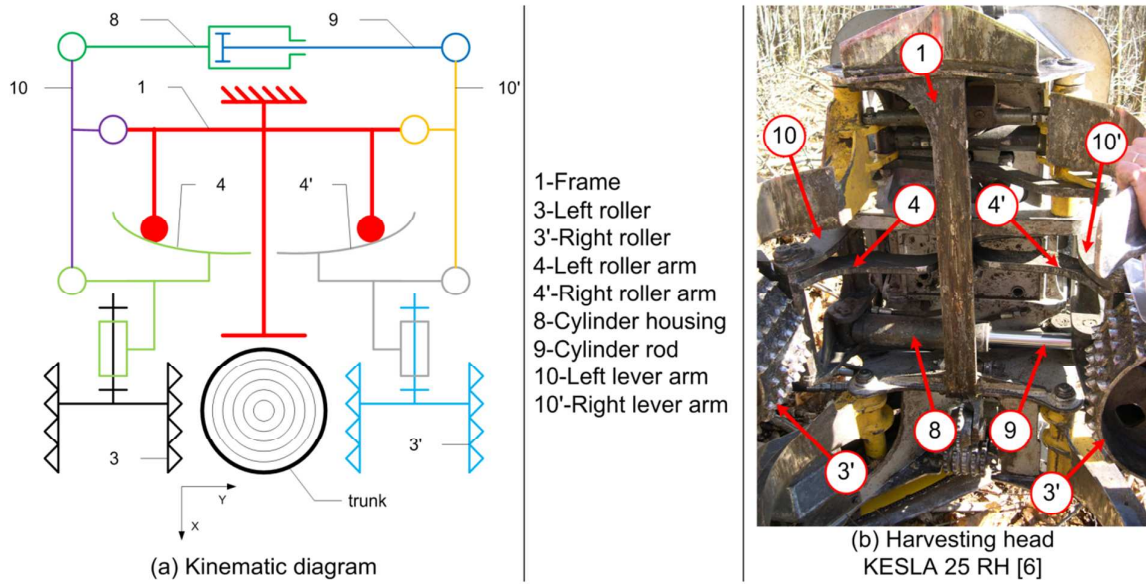


Figure 17: Rollers moved by a cam gripping mechanism

3.3.2 Symmetrically balanced gripping mechanism

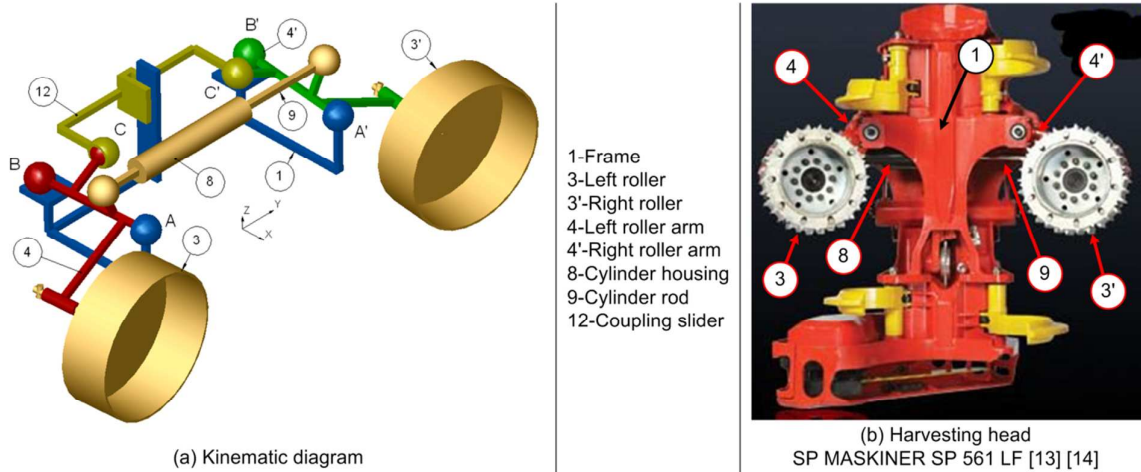


Figure 18: Roller arms moved by a symmetrically balanced gripping mechanism

Contrary to the previous ones, this hybrid gripping mechanism has a structure which makes it move symmetrically with respect to the (X, Z) plane. Such a mechanism is able to fulfill a centering function. It will be studied in detail in section 4.

4 Structural analysis of the symmetrically balanced gripping mechanism

This section presents the study of the patented gripping mechanism described in the previous section (Figure 18). Assimilating this mechanism to a parallel mechanism, this study will be lead by using the structural parameters and corresponding formulae established by the third author of this paper [15].

At first, we will introduce the structural graph of this mechanism. Then we will lead a structural analysis in three steps. The first one deals with the graph simplification by analyzing the limb corresponding to the actuator. In the second step, we will suppress an internal loop created by two “in parallel assembled” pairs. And the structural parameters will be calculated in the third step.

4.1 Structural graph of the mechanism

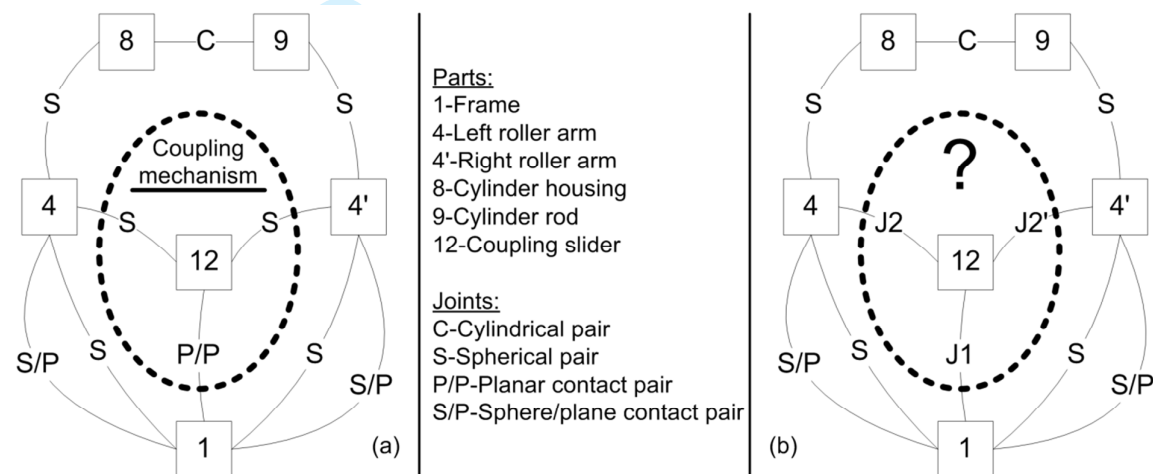


Figure 19: Structural graph of the mechanism

Figure 19-a represents the structural graph of the studied mechanism. The parts are symbolized by the squares and the joints by the edges between the squares. The surrounded sub-chain corresponds to the coupling mechanism allowing the symmetric motion of the right and left roller arms.

After having performed the structural analysis of the whole mechanism, in the section 5, we will execute a structural synthesis of the coupling sub-chain in order to find all the existing combinations of joints J_1 , J_2 and J_2' which do not change the whole mechanism behavior (Figure 19-b). By symmetry, we consider that J_2 and J_2' are similar joints.

4.2 Structural analysis

4.2.1 Influence of the limb combining the actuator

The whole mechanism can be considered as a parallel mechanism. It can be divided in two parts: the limb G_a combining the linear actuator and the “unactuated” mechanism surrounded with the dotted line (Figure 20). The limb G_a consists of two spherical pairs, a cylindrical pair and two parts 8 and 9.

The parameters belonging to the unactuated mechanism will be appended by a “u” index and the parameters referring to the limb G_a will be appended with a “a” index.

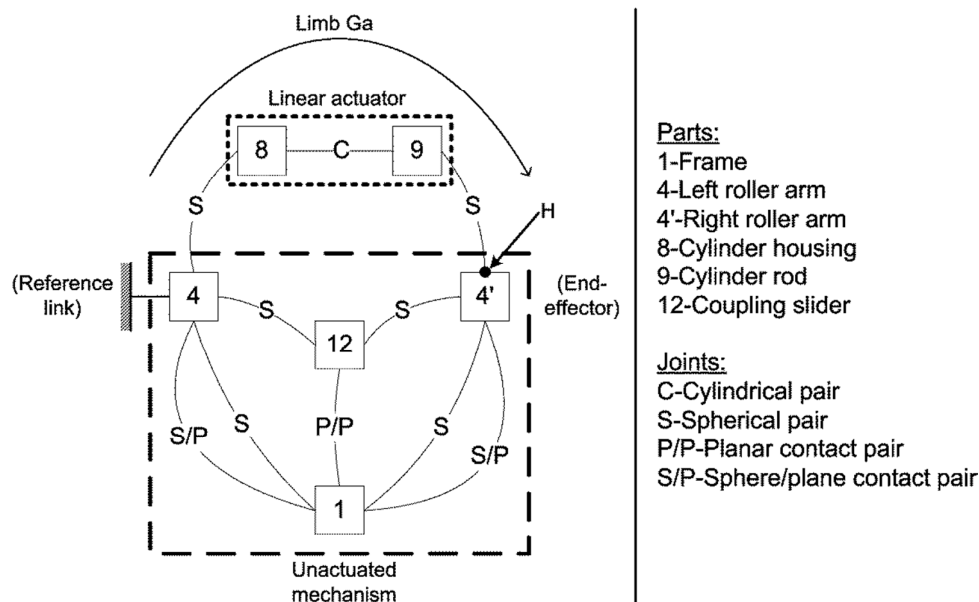


Figure 20: The limb combining the actuator

In order to study the influence on the structural parameters of the limb G_a , we will consider the left roller arm (4) as the reference link and the right roller arm (4') as the end effector.

By opening the limb G_a in H, we can see that point H can move long each axis and rotate around each axis without dependencies between the motions. Then the basis of the relative velocities vector space of this limb G_a is $R_a = \{\overline{Vx}, \overline{Vy}, \overline{Vz}, \overline{\omega x}, \overline{\omega y}, \overline{\omega z}\}$ and the connectivity S_{Ga} between (4) and (4') is equal to 6 ($S_{Ga} = 6$). So, regardless of the connectivity $(S_F)_u$ of the end effector (4') in the unactuated mechanism, the intersection $R_a \cap (R_F)_u$ is $(R_F)_u$ and then the connectivity $(S_F)_u$ of the end effector is not altered by the limb G_a .

$$S_F = (S_F)_u \quad (\text{eq. 1})$$

The internal loops of the structural graph are also not modified by the limb G_a .

$$r_l = (r_l)_u \quad (\text{eq. 2})$$

The number of joint parameters (r) that lost their independence in the loop closure of the whole mechanism is given by the following formula [15]:

$$r = \sum_{\text{whole mechanism}} S_{Gi} - S_F + r_l \quad (\text{eq. 3})$$

By decomposing the sum of the limb connectivities into the one belonging to the limb G_a and the others belonging to the unactuated mechanism, we can write:

$$r = \sum_{\text{unactuated}} S_{Gi} + S_{Ga} - S_F + r_l \quad (\text{eq. 4})$$

By including equations 1 and 2, and $S_{Ga} = 6$, we obtain :

$$r = r_u + 6 \quad (\text{eq. 5})$$

The mobility of the whole mechanism is defined by [15]:

$$M = \sum_{\text{whole mechanism}} f_i - r \quad (\text{eq. 6})$$

By decomposing the sum of the DOF of each joint into the ones belonging to the limb G_a and the others belonging to the unactuated mechanism, we can write:

$$M = \sum_{\text{unactuated}} f_i + \sum_{\text{actuator}} f_i - r \quad (\text{eq. 7})$$

By calculating the sum of the DOF of each joint in the limb G_a :

$$\sum_{\text{actuator}} f_i = 2 \times f_{(S)} + f_{(C)} = 2 \times 3 + 2 = 8 \quad (\text{eq. 8})$$

So, by including equations 2 and 8 in equation 7, we obtain:

$$M = M_u + 2 \quad (\text{eq. 9})$$

The number of overconstraints in the whole mechanism is given by [15]:

$$N = 6 \times q - r \quad (\text{eq. 10})$$

The limb G_a adds one independent loop to the unactuated mechanism:

$$q = q_u + 1 \quad (\text{eq. 11})$$

By including equations 5 and 11 in the formula 10, we can find:

$$N = N_u \quad (\text{eq. 12})$$

The number of redundancies in the whole mechanism is calculated with the following equation [15]:

$$T = M - S_F \quad (\text{eq. 13})$$

So, using equations 1 and 9 this formula becomes:

$$T = T_u + 2 \quad (\text{eq. 14})$$

To summarize the results linking the structural parameters of the whole mechanism to the unactuated mechanism, the following relations are obtained:

$$\begin{cases} r = r_u + 6 \\ M = M_u + 2 \\ N = N_u \\ T = T_u + 2 \end{cases} \quad (\text{eq. 15})$$

In order to simplify the study, the structural analysis will focus on the unactuated mechanism. Knowing the previous results and the values of each structural parameter belonging to the unactuated mechanism, it will be easy to calculate the structural parameters of the whole mechanism.

4.2.2 Simplification by replacing the internal loops by equivalent serial chains

The structural graph of the unactuated mechanism contains two internal loops which make the calculus more difficult. These two internal loops are similar because of the symmetry of the mechanism. Each loop is composed of two joints S/P and S linking the two same parts 1 and 4 (respectively 1 and 4').

These two joints allow the arm 4 (respectively 4') to rotate around two axes: the Z axis and the axis defined by points A and B (respectively A' and B'). An equivalent serial kinematic chain can be obtained by using two revolute pairs in serial connected with an additional part 13 (respectively 13'). This modification is shown by the kinematic diagram in Figure 21-d.

The resulting structural graph has no more internal loop (Figure 21-b).

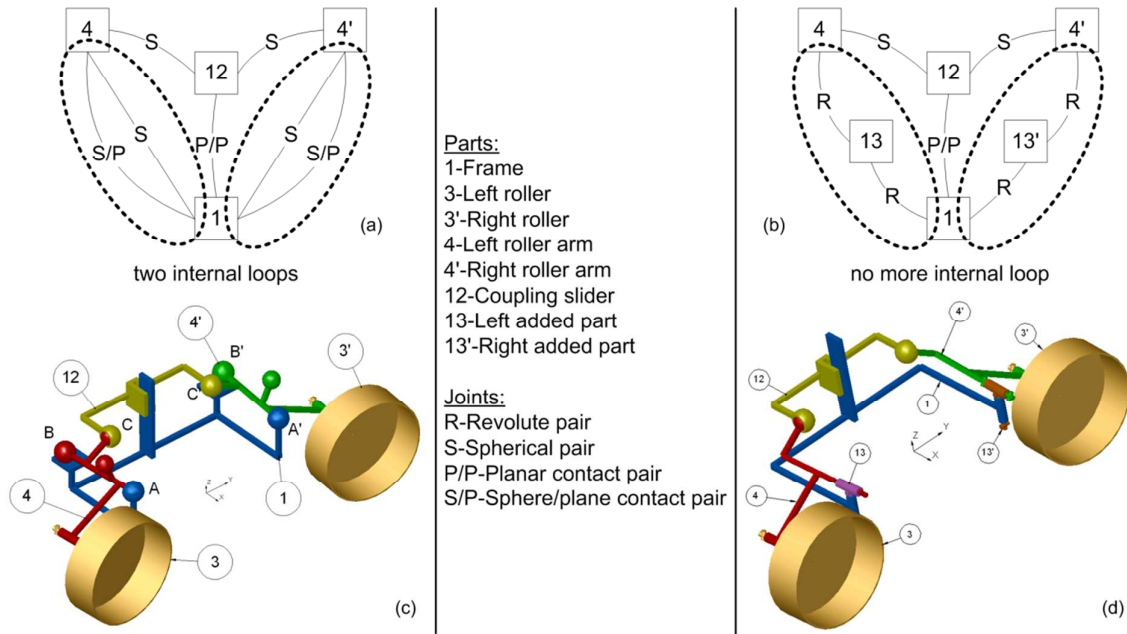


Figure 21: Equivalent kinematic chains

4.2.3 Structural parameters

After the successive simplifications, we can now easily perform the calculation of the structural parameters. Let us consider part 1 as the base of the simplified unactuated mechanism and part 12 as its end-effector. This mechanism has three limbs G_1 , G_2 and G_2' , as shown in Figure 22-a.

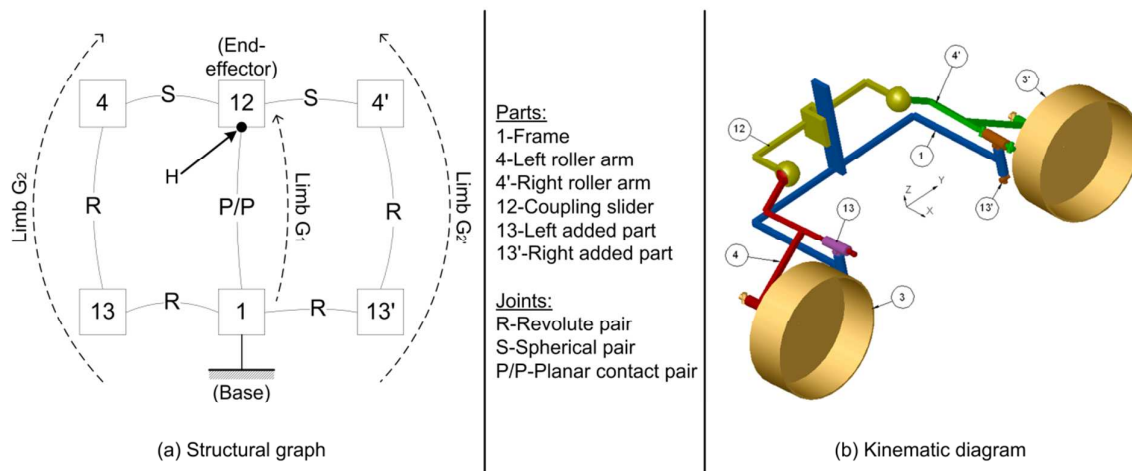


Figure 22: Simplified unactuated mechanism

Let us open the three limbs in H.

The independent velocity vector space for the limb G_1 is given by the mobility of the planar contact pair (P/P):

$$R_{G_1} = \{\vec{V}_x; \vec{V}_z; \vec{\omega}_y\} \tag{eq. 16}$$

The connectivity of part 12 through the limb G_1 is

$$S_{G_1} = 3 \tag{eq. 17}$$

The independent velocity vector spaces for the limbs G_2 and $G_{2'}$ are not fixed. The connectivity of part 12 through each limb is 5 and all the mobilities are permitted. So, we can choose any vector space with a dimension of 5.

$$S_{G_2} = S_{G_{2'}} = 5 \quad (\text{eq. 18})$$

The connectivity $(S_F)_u$ of the end-effector, when all the limbs are linked to it, is defined by the dimension of the velocity vector space given by the minimal intersection of the respective velocity vector spaces R_{G_i} of minimal dimension.

$$(S_F)_u = \text{MIN}(\text{dim}(R_F)) = \text{MIN}(\text{dim}(R_{G_1} \cap R_{G_2} \cap R_{G_{2'}})) \quad (\text{eq. 19})$$

In order to obtain this minimal dimension, both R_{G_2} and $R_{G_{2'}}$ contain the vectors \vec{V}_Y , $\vec{\omega}_X$ and $\vec{\omega}_Z$. Their two last vectors must be chosen among the vectors of R_{G_1} . So, R_{G_2} and $R_{G_{2'}}$ always have minimum one in common vector, which is also in R_{G_1} . Then, the minimal dimension of the intersection is 1.

$$(S_F)_u = 1 \quad (\text{eq. 20})$$

Now we are able to calculate:

$$r_u = S_{G_1} + S_{G_2} + S_{G_{2'}} - (S_F)_u = 12 \quad (\text{eq. 21})$$

the mobility:

$$M_u = 4 \times f_{(R)} + 2 \times f_{(S)} + f_{(P/P)} - r_u = 1 \quad (\text{eq. 22})$$

the number of overconstraints:

$$N_u = 6 \times q_u - r_u = 0 \quad (\text{eq. 23})$$

and finally, the redundancy:

$$T_u = M_u - (S_F)_u = 0 \quad (\text{eq. 24})$$

The following parameters are obtained by summarizing these results:

$$\begin{cases} r_u = 12 \\ M_u = 1 \\ N_u = 0 \\ T_u = 0 \end{cases} \quad (\text{eq. 25})$$

5 Structural synthesis of equivalent spatial gripping mechanisms

This section presents the structural synthesis of the coupling sub-chain surrounded in Figure 19. The aim of this synthesis is to find all the couples of joints (J1; J2) which can replace the actual joints without changing the mechanism behavior (Figure 23). After the determination of the combinations of joints respecting the hypotheses, we will illustrate these structural results with corresponding examples of kinematic diagrams.

5.1 Structural synthesis of the coupling sub-chain

The mobility, the number of overconstraints and the redundancies must stay the same.

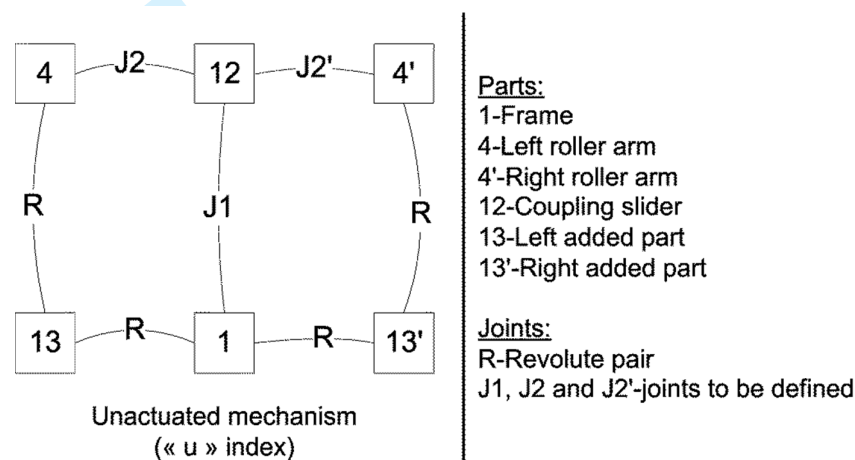


Figure 23: The simplified structural graph with unknown joints J1, J2 and J2'

The mechanism being non-overconstrained, and the number of independent loops being 2, we still have:

$$r_u = N_u + 6 \times q_u = 12 \quad (\text{eq. 26})$$

Then, by expressing the unactuated mechanism mobility as a function of the number of degrees of freedom in joints J1, J2 and J2', we obtain:

$$M_u = 4 \times f_{(R)} + f_{(J1)} + f_{(J2)} + f_{(J2')} - r_u \quad (\text{eq. 27})$$

Joints J2 and J2' being of the same type have the same degree of freedom. Moreover, the revolute pair has only one degree of freedom. Finally, the unactuated mechanism mobility is still equal to 1.

So, we can write:

$$f_{(J1)} + 2 \times f_{(J2)} = 9 \quad (\text{eq. 28})$$

Then, knowing that $f_{(J1)}$ is an integer between 0 and 6, we obtain a finite number of combinations for $f_{(J1)}$ and $f_{(J2)}$.

In order to choose joints J1 and J2 with their number of degrees of freedom, we use the following table:

Table 1: List of joints and their respective number of degrees of freedom

symbole	name	Number of degrees of freedom: $f_{(J_i)}$
R	revolute	1
P	prismatic	1
C	cylindrical	2
S	spherical	3
P/P	planar contact	3
S/C	sphere / cylinder contact	4
C/P	cylinder / plane contact	4
S/P	sphere / plane contact	5

The following table presents the possible combinations for the two joints:

Table 2: Possible combinations for joints J1 and J2.

$f_{(J_1)}$	possibilities for J1	$f_{(J_2)}$	possibilities for J2	number of combinations (J1,J2)
1	2 (P or R)	4	2 (C/P or S/C)	4
3	2 (S or P/P)	3	2 (S or P/P)	4
5	1 (S/P)	2	1 (C)	1
			TOTAL	9

Thereby, the structural synthesis gives us a total of nine combinations. Each of these nine possibilities can themselves generate more than one mechanism by playing on joint orientation. The next section illustrates the results of the structural synthesis by presenting some examples of kinematic diagrams in which the joint orientation has been chosen arbitrarily.

In the obtained mechanisms, the number of kinematic joints constituting the coupling sub-chain is the same as the original one. But, it would be interesting to study the possibilities to replace some joints by equivalent kinematic chains without changing the structural parameters of the initial mechanism.

5.2 Examples of kinematic diagrams

The following figures give some examples of possible kinematic diagrams corresponding to the combinations of joints (J1, J2) found through the structural synthesis.

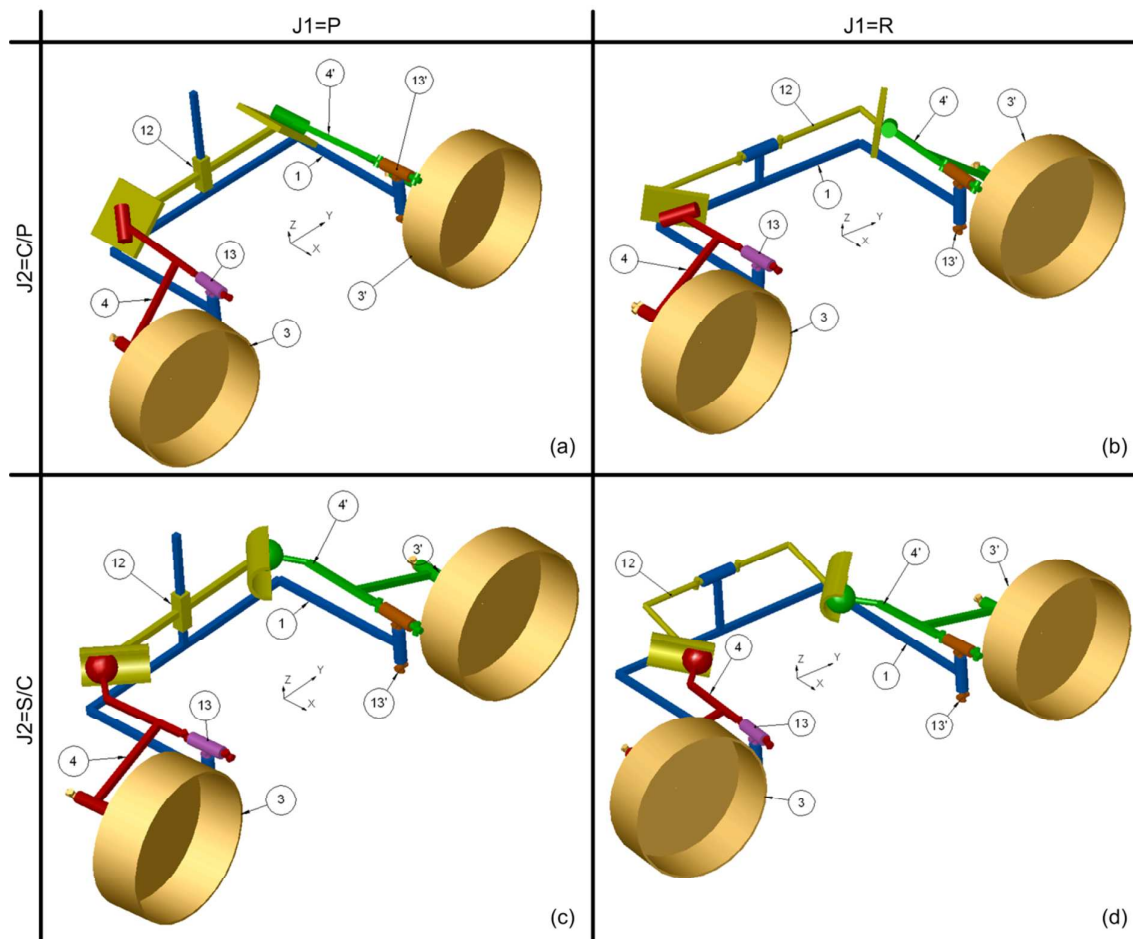


Figure 24: Examples of kinematic diagrams with $J1=P$ or R and $J2=C/P$ or S/C

The original mechanism has a symmetry relative to the plane (X, Z) passing through the middle of the segment AA' (Figure 18-a). Its motions are also symmetrical relatively to this same plane. If we want to preserve this behavior and this geometric particularity, the positioning of joints is not completely arbitrarily. For example, let us consider joint $J1$ which is on the symmetry plane. If we decide that it becomes a revolute joint (R), the axis of this joint must be perpendicular to symmetry plane. The symmetry is also geometrically respected if the joint axis is included in the plane, but the resulting motions of part 12 are not symmetric relatively to this plane.

The result is not the same with a prismatic joint (P). This joint is defined by a direction which must be included in the symmetry plane in order to preserve the geometric and the behavior symmetries. In fact, if this direction is perpendicular to the symmetry plane, part 12 does not have a symmetric motion relatively to this plane.

After having note this rules, a geometric optimization is needed in order to choose the right distance between the revolute pair axis and point C along the X axis or to choose the optimum orientation of the prismatic pair axis around the Y axis.

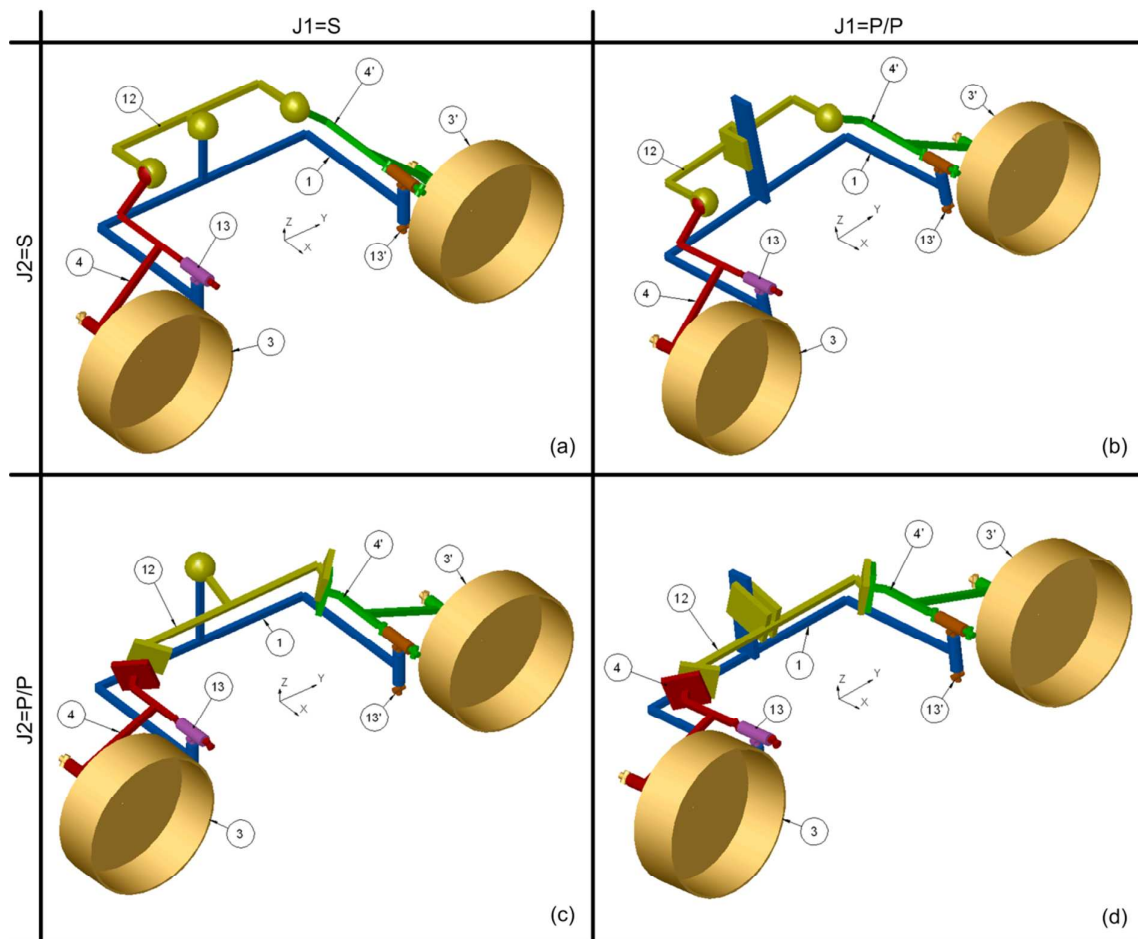


Figure 25: Examples of kinematic diagrams with $J1=S$ or P/P and $J2=S$ or P/P

Still considering joint $J1$, the geometric conclusions concerning the spherical joint (S) is not so obvious (Figure 25-a and c). A spherical pair consists of three rotations whose respective axes are convergent. So, there are always some of these axes which are not perpendicular to the symmetric plane. Then the behavior symmetry is not verified except if the two rotations are locked by the kinematic constraints given by the other joints.

If we replace the two joints $J2$ and $J2'$ by two spherical joints (Figure 25-a and b), part 12 can rotate around the axis going through the two centers of these spherical joints. If this potential rotation is not locked by joint $J1$, then the mechanism has a new internal mobility. This phenomenon happens especially in the kinematic diagram shown in Figure 25-b when the considered rotation axis of part 12 is perpendicular to the plane defining the planar contact joint (P/P) in $J1$. This phenomenon also happens when the center of the spherical joint (S) in $J1$ is on the considered rotation axis of part 12 (Figure 25-a).

Let us consider now the case in which joints $J1$, $J2$ and $J2'$ are all replaced by a planar contact joint (P/P) (Figure 25-d). A planar contact pair fixes the direction of a rotation axis, which is perpendicular to its plane. For joint $J1$, we have explained before that this rotation axis must be perpendicular to the symmetry plane to obtain the behavior symmetry of the mechanism. If it is not, the parasitic rotations must be locked by the global kinematic behavior of the mechanism. By placing the planar contact pair in order to make the direction of the rotation axis perpendicular to the symmetry plan, the plane defining the planar contact pair coincides with the symmetry plane. Let us name this solution "solution 1".

On the other hand, the planes defining the planar contact joints in $J2$ and $J2'$ have a common intersection line, except if they are parallel. But this parallelism coupled with the solution 1 introduces three extra mobilities: that is what we do not want. So, let us go back to the intersection line which is necessarily on the mechanism symmetry plane. If we do not want to generate an additional mobility, this line must not be parallel to the plane defining the planar contact joint located in $J1$. This new solution is not compatible with the “solution 1” established before. So, as a conclusion, the planar contact joint located in $J1$ must be oriented in order to have its rotation axis included in the mechanism symmetry plane. This rotation axis is only oriented in the planar contact pair, but it is not fixed. So, the global mechanism behavior must keep this axis in the symmetry plane and lock the corresponding rotation in order to preserve the behavior symmetry.

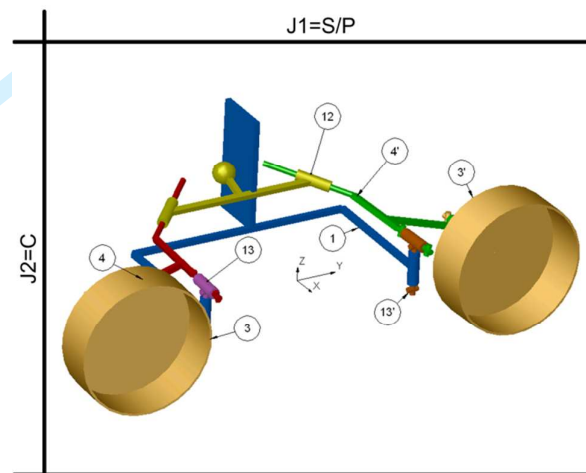


Figure 26: Example of kinematic diagram with $J1=S/P$ and $J2=C$

Considering now the case where joint $J1$ is replaced by a sphere-plane contact joint and joints $J2$ and $J2'$ are each replaced by a cylindrical joint (C) (Figure 26). The rotation and translation axis defining the cylindrical pair must be well oriented in order to prevent undesirable internal mobilities. For example, if this rotation axis of $J2$ (respectively $J2'$) coincides with the rotation axis defining the revolute joint (R) between parts 3 and 13 (respectively parts 3' and 13'), the roller arms 4 (respectively 4') can rotate independently around this common axis: we have two extra mobilities in this case. On the other hand, if the rotation axis of $J2$ (respectively $J2'$) is parallel to the rotation axis defining the revolute joint between parts 1 and 13 (respectively parts 1 and 13'), the loop consisting of parts 1-13-4-12-4'-13'-1 behaves like a four bar linkage. The resulting motion of the two roller arms is not symmetric, regardless of the joint orientation located in $J1$.

6 Conclusion

This paper is an extended version of [18] consisting of two main parts. The first one deals with the state of the art about the gripping function used in wood harvesting devices. After a short definition of the wood harvesting activities, this part presents the progressive mechanization of the devices used up to now. Then the current all-in-one harvesting heads are described in terms of components and functions. This description allows emphasizing the significant role of the gripping function in this kind of devices. Different existing marketed designs are presented, each one with an example of existing harvesting head and the corresponding kinematic diagram. Those mechanisms can grip with a concentric/lateral and a symmetric/non-symmetric motion of the arms.

The second part focuses on a patented and marketed hybrid gripping mechanism combining the advantages of concentric and lateral gripping. This one is able to generate a symmetric motion of the gripping components between the left and the right sides of the head. Considering such a mechanism like a parallel one and after two steps of simplification concerning the actuator and the internal loops, its structural analysis is performed. Then, a structural synthesis of the sub-chain coupling the side component motions, allows finding a total of nine combinations of joints preserving the structural parameter values of the original mechanism. Finally, these nine results are each illustrated through an example of corresponding kinematic diagram with a short review.

This study shows a particular method that can be followed in order to perform a structural synthesis. This method works in the structural domain and allows finding structural solutions: the result is only expressed in terms of type of joints. Afterwards, it is necessary to translate this result into a kinematic solution by choosing the right pose of each joint in a similar way as [19] and [20]. The number of combinations can be thereby seriously increased.

The path from the structural description to the kinematic diagram requires a geometric study of the existing joints and their associated geometric skeleton. Further work will allow to position and orientate the skeleton of each joint in space in order to obtain a functioning kinematic diagram.

Acknowledgments

This research work is part of FUI ECOMEF project funded by Conseil Régional Auvergne and FEDER – “Europe en Auvergne”. These organisms are acknowledged for their financial support.

References

- [1] STIHL. MS 660 motorized chain saw technical description (web site). <http://www.stihl.fr/Produits-STIHL/Tron%C3%A7onneuses/Tron%C3%A7onneuses-pour-travaux-forestiers/2475-131/MS-660.aspx>, 2012
- [2] ARMEF. SIFER 103 C technical description. Annales de mécanisation forestière 1983. ARMEF, 1984, p. 33
- [3] JOHN DEERE. Harvesting heads, H200 series (booklet). http://www.deere.fr/fr_FR/docs/product/equipment/harvesting_heads/john_deere/h200_series/brochures/brochure_h200_series.html, 2012
- [4] JOHN DEERE. Harvester 1070R/1170E (booklet). http://www.deere.fr/fr_FR/docs/product/equipment/wheeled_harvesters/1170e/brochures/brochure_1070e_1170e.html, 2012
- [5] Laurier J.P. Mechanization of wood harvesting in France: state of the art in 2009. Forêt Entreprise, 2010
- [6] KESLA. Harvester heads (booklet). <http://www.kesla.fi/documents/10304/10580/KESLA+harvester+head+ENG.pdf>, 2012
- [7] KOMATSU. KOMATSU 370.2 harvesting head technical description (booklet). http://shop.mediahandler.se/pdf/komatsu/k370_2_ps_gb.pdf, 2012
- [8] PONSSE. PONSSE H8 harvesting head technical description (booklet). http://www.ponsse.com/content/download/3832/111350/file/H8_ENG.pdf, 2012
- [9] JOHN DEERE. Harvesting heads, H400 series (booklet). http://www.deere.fr/fr_FR/docs/product/equipment/harvesting_heads/john_deere/h400_series/brochures/brochure_h400_series.html, 2012
- [10] LOGMAX. Log Max 7000C harvesting head technical description (booklet). http://www.logmax.com/pdf/7000/Log_Max_Prod_7000C_English.pdf, 2012
- [11] KETONEN. Keto 600 TS harvesting head technical description (booklet). <http://www.kone-ketonen.fi/MalliDokumentit/KETO%20600%20TS/KETO%20600%20Eng.pdf>, 2012
- [12] Ketonen L. Tree trunk feed mechanism. Patent SE 455283, 1988
- [13] SP MASKINER. SP 561 LF harvesting head technical description (booklet). <http://www.spmaskiner.se/en-gb/pdf/folder-sp561lf.pdf>, 2012
- [14] Johansson A. Single grip harvester head felling and processing of trees. Patent WO 98/54949, 1998
- [15] Gogu, G. Structural synthesis of parallel robots. Part 1: Methodology. Springer, 2008
- [16] AFNOR. NF EN ISO 3952-1: Kinematic diagrams – graphical symbols – Part 1. AFNOR, 1995
- [17] IFToMM. Dictionaries online. http://www.iftomm.3me.tudelft.nl/1036_2057, 2010
- [18] Goubet D, Fauroux J.C., Gogu G. Structural Synthesis of Innovative Gripping Mechanisms for Wood Harvesting. New Trends in Mechanism and Machine Science. Edited by Fernando Viadero and Marco Ceccarelli, Springer, Mechanisms and Machine Science, Vol. 7, 2012, pp. 663-670

- 1
2
3 [19] Ravisankar R., Mruthyunjaya T. S. Computerized synthesis of the structure of geared kinematic chains.
4 Mechanism and Machine Theory, 1985, Vol. 20, No 5, pp. 367-387
5
6 [20] Soni A. H., Mohammad H. F. Dado, Weng Yicheng: An Automated Procedure for Intelligent
7 Mechanism Selection and Dimensional Synthesis. Journal of Mechanisms, Transmissions, and
8 Automation in Design, 1988, Vol 110, pp. 130-137
9
10
11
12
13
14
15
16
17
18
19
20
21
22
23
24
25
26
27
28
29
30
31
32
33
34
35
36
37
38
39
40
41
42
43
44
45
46
47
48
49
50
51
52
53
54
55
56
57
58
59
60

For Review Only

Appendix 1: kinematic pairs

The table of Figure 27 lists the kinematic pairs used in this paper, according with the norm ISO 3952-1 [16] and the IFToMM terminology [17].

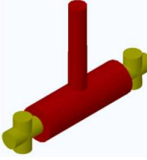

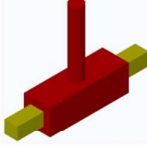

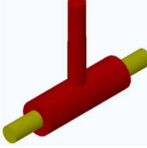



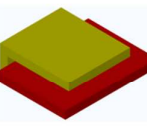
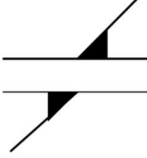
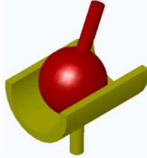

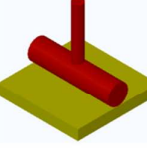
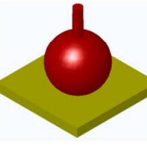
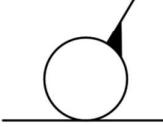
Name	3D diagram	2D diagram	Code	DoF
Revolute pair			R	1
Prismatic pair			P	1
Cylindrical pair			C	2
Spherical pair			S	3
Planar contact pair			P/P	3
Ball and cylinder pair or sphere-cylinder contact pair			S/C	4
Cylinder-plan contact pair			C/P	4
Ball and plan pair or sphere-plan contact pair			S/P	5

Figure 27: Kinematic pairs used in this paper

Appendix 2: structural parameters

The following formulae are proposed in [15] for the calculation of the structural parameters of a parallel mechanism:

$$M = \sum_{i=1}^p f_i - r \quad (\text{eq. 29})$$

$$r = \sum_{i=1}^k S_{Gi} - S + r_l \quad (\text{eq. 30})$$

$$N = d q - r \quad (\text{eq. 31})$$

$$T = M - S \quad (\text{eq. 32})$$

M designates the mobility. It represents the number of kinematic parameters to be defined to fix the position of the mechanism. p is the number of joints in the mechanism. f_i represents the degree of freedom in the joint i .

For closed loop mechanisms, r represents the number of joint parameters that lose their independence in the loop closure. k is the number of limbs in the mechanism. S_{Gi} is the connectivity between the last link of the open kinematic chain Gi and the body, before closure. S is the connectivity between the link joining all the mechanism limbs and the body. r_l is the sum of the r values generated by the internal loops of the different limbs of the mechanism.

N is the number of overconstraints. $d=3$ for 2D and $d=6$ for 3D. q is the number of independent loops in a multi-loop mechanism given by Euler's formula $q = p - m + 1$, where p is the number of joints and m the number of links in the mechanism.

T is the structural redundancy.